Observation of Optical Mixing Due to Conduction Electrons in n-Type Germanium

Charles C. Wang and N.W. Ressler
Scientific Research Staff, Ford Motor Company, Dearborn, Michigan 48121
(Received 10 April 1970)

This paper reports the first observation of the optical mixing due to conduction electrons in n-type germanium. The measured magnitude and anisotropy of the third-order susceptibilities are found to be in good agreement with the nonparabolicity effect calculated with a $\vec{k}\cdot\vec{p}$ method involving eight bands at the L point in the reciprocal lattice. It is concluded that the mechanism of momentum-dependent relaxation times contributes negligibly to the observed nonlinearity.

Optical mixing due to conduction electrons in semiconductors has been the subject of several recent publications.[1-7] In GaAs and other III-V semiconductors,[1,2] it has been found that both bound (valence) electrons and conduction electrons contribute to the observed nonlinearity. It appears certain that the conduction-electron nonlinearity observed in these semiconductors arises from the momentum-dependent effective mass (nonparabolicity effect) of the conduction electrons,[3-5] rather than the momentum-dependent relaxation times[6,7] of these electrons. However, no optical mixing attributable to conduction electrons has hitherto been observed in the elemental semiconductors Si and Ge. The purpose of this paper is to report the first observation of optical mixing due to the conduction electrons in n-type Ge samples. The measured magnitude and anisotropy of the third-order susceptibilities are found to be in reasonable agreement with the nonparabolicity effect calculated with a $\vec{k}\cdot\vec{p}$ calculation involving eight bands at the L point in the reciprocal lattice. It is concluded that the relaxation-time mechanism contributes negligibly to the observed conduction-electron nonlinearity in Ge.[8]

The experimental setup used to measure the third-order nonlinearities is similar to that employed by previous workers,[1,2] and is shown schematically in Fig. 1. Two CO_2 lasers, frequency selected to lase at 9.6 μ (ω_a) and 10.6 μ (ω_b), respectively, were synchronously Q switched to emit light pulses about 300 nsec in duration. The output from the two lasers were made collinear through a 50% beam splitter and then amplified using a 2-m CO_2 laser amplifier. The output from the amplifier, with about 5 kW in each line, was focused onto the sample with a 25-cm BaF_2 lens. The signal generated at the combination frequency of 8.7 μ ($\omega_3 = 2\omega_a - \omega_b$) was then passed through a $\frac{1}{2}$-m Jarrell-Ash spectrometer, detected with a copper-doped Ge detector, and averaged with a Brookdeal boxcar integrator.

The [1$\bar{1}$0] slices of germanium were obtained from Eagle-Pitcher in 5 mm thicknesses. The carrier density was deduced from Hall-effect measurements, assuming that the Hall and conductivity mobilities were the same. The results were found to be consistent with the resistivity measurements quoted by the supplier. The samples with $n = 1.1 \times 10^{14}$ and 2.1×10^{17} were polished and the two faces made parallel to within 2 min of arc. The parallelism for these two samples was made to facilitate the anisotropy measurements to be described below. Other samples used had a wedge as large as 15 min. For the combination frequency generation at ω_3, each sample was tilted away from normal incidence by about 20° to avoid complications arising from the presence of channel spectra at the incident and signal frequencies.

Figure 2 shows the relative values of the square of the third-order coefficient for Ge sam-

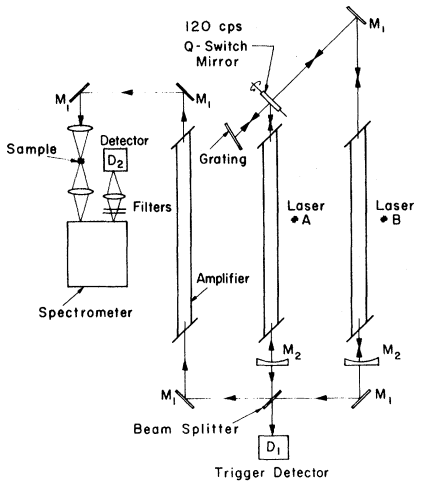

FIG. 1. Schematic of the experimental setup. M_1 are totally reflecting mirrors.

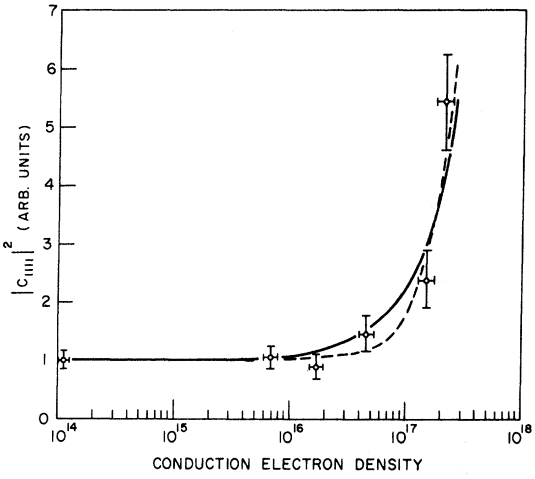

FIG. 2. Dependence of $|c_{1111}|^2$ as a function of carrier concentration. The solid curve is a plot of $(1+bn)^2$ with $b=0.5\times10^{-17}$, and the dashed curve is a plot of $1+(b'n)^2$ with $b'=0.85\times10^{-17}$. These represent, respectively, the case when the conduction-electron nonlinearity adds in phase (solid curve) to the valence-electron nonlinearity, and the case when the two nonlinearities add in quadrature (dashed curve).

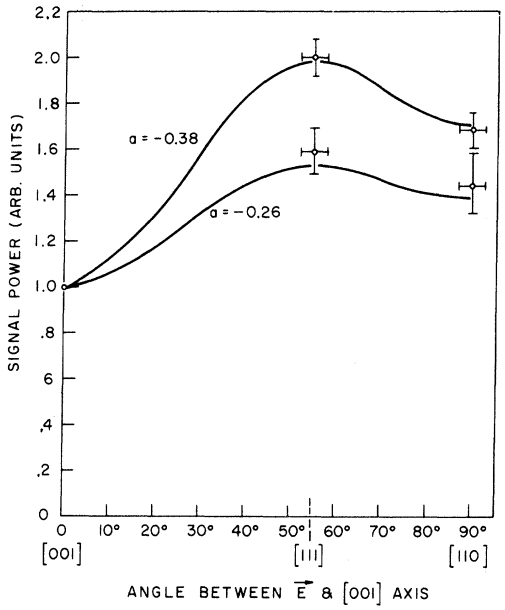

FIG. 3. Angular dependence of the signal power generated at the combination frequency ω_3 from the intrinsic sample (upper data points) and from the sample with $n=2.1\times10^{17}$ cm^3 (lower data points). The upper curve is a best fit using Eq. (2), and the lower curve is a plot of Eq. (2) with $a=-0.26$.

ples with varying carrier concentration. These values were deduced from measurements of the signal power at ω_3 with the $\vec{E}$ fields polarized along the [001] crystal direction, taking into account the losses due to free-carrier absorption. The measured signal power actually decreases with increasing carrier concentration because of the rapid onset of free-carrier absorption. The absorption constant was measured for all samples at the wavelengths of interest. This and other parameters used to deduce the third-order coefficients[2] are given in Table I.

Figure 3 shows the relative signal power generated in the intrinsic sample, and the sample No. 6 with $n=2.1\times10^{17}$ cm^3 as the direction of the $\vec{E}$ field relative to the crystal axis is varied. The error bars reflect the mean deviation of the signals from the four equivalent [111] directions, the two equivalent [110] directions, and the two equivalent [001] directions which occur in a $[1\bar{1}0]$ plane.

For a crystal with cubic symmetry, the third-order nonlinear polarization induced at the combination frequency $\omega_3=2\omega_a-\omega_b$ is given phenomenologically by[9]

$$P_i^{(3)}=3c_{1122}(E_jE_jE_i+aE_jE_jE_i\delta_{ij}) \quad . \tag{1}$$

Here $a=(c_{1111}/3c_{1122})-1$; c_{1122} and c_{1111} are the two independent components of a fourth-rank tensor; the coefficient a is a measure of the degree of anisotropy[10]; $a=0$ (and hence $3c_{1122}=c_{1111}$) for an isotropic medium. With the incident $\vec{E}$ fields polarized in a $[1\bar{1}0]$ plane, the resulting signal power at ω_3 is given by

$$W^{(3)}(\omega_3)\propto\left|(3c_{1122})^2[1+a(2\cos^4\theta+\sin^4\theta)+a^2(\cos^6\theta+\tfrac{1}{4}\sin^6\theta)]\right| \quad , \tag{2}$$

where θ is the angle between the [001] axis in the

TABLE I. Parameters used to deduce the value of $|c_{1111}|^2$ in Fig. 2 from the measured power at ω_3. l is the sample thickness, α is the measured absorption coefficient, $\Delta k=2k_\alpha-k_b-k_3$.

Sample	N(cm^{-3})	l (mm)	$\alpha(8.7\mu)$	$\alpha(9.6\mu)$	$\alpha(10.6\mu)$	Δk(cm^{-1})
1	1.1×10^{14}	3.96	0	0	0	−1.7
2	6.9×10^{15}	4.88	0	0	0	−1.7
3	1.7×10^{16}	4.73	0.23	0.29	0.42	−1.7
4	4.5×10^{16}	3.96	0.55	0.70	0.83	−0.9
5	1.5×10^{17}	4.95	2.3	2.6	3.2	−0.6
6	2.1×10^{17}	3.96	3.3	4.1	5.0	−0.3

plane and the direction of the $\vec{E}$ fields.

For intrinsic samples, one deduces from the upper curve[11] of Fig. 2 that $a = -0.38 \pm 0.02$. For more heavily doped samples, it is seen from Fig. 3 that the angular dependence of the signal power is markedly different. For the sample with $n = 2.1 \times 10^{17}$ cm^{-3}, one finds that $a = -0.28 \pm 0.05$. This difference in the anisotropy is clear evidence for the presence of the conduction-electron nonlinearity. Analysis of the data in Fig. 2 further indicates that in the sample No. 6 this additional nonlinearity is responsible for about $(60 \pm 10)\%$ of the observed power at ω_3. The uncertainty in the percentage reflects our inability to determine whether the conduction- and valence-electron nonlinearities add in phase or in quadrature.

As an estimate of the conduction-electron nonlinearity due to the nonparabolicity effect, we have employed the $\vec{k} \cdot \vec{p}$ perturbation approach[12] and the band parameters[13] available for Ge to calculate to fourth order the ϵ-versus-$\vec{k}$ relation near the conduction-band edge L_1:

$$\epsilon(\vec{k}) \cong \epsilon_0 + (\hbar^2/2m_{\parallel})k_{\parallel}^2 + (\hbar^2/2m_{\perp})k_{\perp}^2 - \tfrac{1}{4}(\hbar^4/m_{\perp}^2 E_g)(1 - m_{\perp}/m_0)^2 \times (1.4k_{\perp}^4 + 0.8k_{\parallel}^2 k_{\perp}^2 + 0.005k_{\parallel}^4) \quad . \tag{3}$$

Here m_0 is the free-electron mass: $E_g \approx 2.2$ eV is the direct-band gap $(L_1 - L_3')$; $m_{\parallel}$ and $m_{\perp}$ are, respectively, the longitudinal and transverse effective masses at the conduction-band edge; and $k_{\parallel}$ and $k_{\perp}$ are, respectively, the longitudinal and transverse components of $\vec{k}$. In arriving at the values in Eq. (3), the spin-orbit coupling has been neglected, and it has been assumed that the momentum matrix elements for the allowed transitions between the eight bands at the L point are the same.[14] Explicit calculation shows that the nonparabolicity in Eq. (3) comes mostly from the coupling between the three bands L_1, L_3', and L_3, so that knowledge of the exact energy value for other band edges is not critical.

The third-order nonlinear polarization due to the nonparabolicity in Eq. (3) is given by[5]

$$P_{\perp}^{(3)}(\omega_3) = \tfrac{3}{4}n(e^4/m_{\perp}^2 E_g \omega_a^2 \omega_b \omega_3)(1 - m_{\perp}/m_0)^2 \times E_a^2 E_b(1.4\sin^3\alpha + 0.4\sin\alpha\cos^2\alpha) \quad ,$$

$$P_{\parallel}^{(3)}(\omega_3) = \tfrac{3}{4}n(e^4/m_{\perp}^2 E_g \omega_a^2 \omega_b \omega_3)(1 - m_{\perp}/m_0)^2 \times E_a^2 E_b(0.4\sin^2\alpha\cos\alpha) \quad , \tag{4}$$

where n is the electron density in the conduction band and α is the angle between the applied fields (E_a and E_b) and the [111] direction under consideration. The corresponding macroscopic coefficients $3c_{1122}(n)$ and $a(n)$ due to the conduction electrons are obtained by averaging Eq. (4) over the four tetrahedrally coordinated conduction-band ellipsoids. Thus, one obtains

$$3c_{1122}(n) = 0.7n(e^4/m_{\perp}^2 E_g \omega_a^2 \omega_b \omega_3) \times (1 - m_{\perp}/m_0)^2 \tag{5}$$

and $a(n) = -0.14$ independently of the conduction-electron density. With $n = 2.1 \times 10^{17}$ cm^3, Eq. (5) gives $3c_{1122}(n) = 0.75 \times 10^{-10}$ esu and $c_{1111}(n) = 3c_{1122}(n)\,[1 + a(n)] = 0.65 \times 10^{-10}$ esu.

It is noted earlier that with $n = 2.1 \times 10^{17}$, the valence and conduction electrons contribute comparably to the observed nonlinearity. Taking as a reference the calculated value of $c_{1111}(n) = 0.65 \times 10^{-10}$ esu for the conduction electrons and assuming that these two contributions add in phase,[5] it follows that c_{1111} (valence) $= 0.65 \times 10^{-10}$ esu for the intrinsic samples of Ge. This value is in reasonable agreement with the value of $(1.2 \pm 0.7) \times 10^{-10}$ esu reported in Ref. 2. Furthermore, by combining the observed anisotropy coefficient for the intrinsic sample and sample No. 6 (Fig. 2), one deduces $a(n) = -0.18 \pm 0.09$ for the anisotropy of the conduction-electron nonlinearity, again in reasonable agreement with the calculated value of -0.14 due to the nonparabolicity effect.

An alternative explanation for the observed conduction-electron nonlinearity is the momentum-dependent relaxation times of the conduction electrons. For the heavily doped sample No. 6, where both acoustic and ionized impurity scattering are present, an upper limit for the relaxation-time nonlinearity is estimated from Eq. (12) of Ref. 5 to be lower than the corresponding nonparabolicity effect by about a factor of 5. In the actual case, the presence of intervalley scattering and scattering by optical phonons tends to further reduce this nonlinearity. One thus expects that the relaxation-time mechanism is probably unimportant in Ge. As a check that this is indeed the case, we have studied the temperature dependence of the signal power at ω_3 in the sample with $n = 2.1 \times 10^{17}$ cm^2. The nonlinearity is expected to be nearly temperature independent for the nonparabolicity effect, but should be sharply temperature dependent for the relaxation-time mechanism.[5] As the temperature was varied between 300 and 110 °K, a factor-of-2 increase in the observed signal power was recorded at the lower temperature. While this increase is consistent with the nonparabolicity effect when the slight reduction in the free-carrier absorption is taken into account, a net decrease by a factor of 2 in the signal power would have been recorded if the relaxation-time mechanism were operative. It is thus concluded that the relaxation-time mech-

anism contributes negligibly to the observed conduction-electron nonlinearity in Ge.

It is a pleasure to acknowledge the many helpful discussions with R. W. Terhune and the invaluable assistance of R. Crain throughout the experiments.

[1]C. K. N. Patel, R. E. Slusher, and P. A. Fleury, Phys. Rev. Letters 17, 1011 (1966).
[2]J. J. Wynne and G. D. Boyd, Appl. Phys. Letters 12, 191 (1968); J. J. Wynne, Phys. Rev. 178, 1295 (1969).
[3]P. A. Wolff and G. A. Pearson, Phys. Rev. Letters 17, 1015 (1966).
[4]S. S. Jha and N. Bloembergen, Phys. Rev. 171, 891 (1968).
[5]C. C. Wang and N. W. Ressler, Phys. Rev. 188, 1291 (1969).
[6]P. Kaw, Phys. Rev. Letters 21, 539 (1968).
[7]B. S. Krishnamurthy and V. V. Paranjape, Phys. Rev. 181, 1153 (1969).
[8]In Ref. 5, the nonparabolicity effect in Ge was assumed negligible. A detailed comparison between these two types of nonlinearities is to be found later in the present paper.
[9]P. D. Maker and R. W. Terhune, Phys. Rev. 137, A801 (1965).
[10]C. C. Wang and E. L. Baardsen, Phys. Rev. 185, 1079 (1969).
[11]Our value of -0.38 ± 0.02 for the ratio $3c_{1122}/c_{1111}$ is somewhat lower than -0.45 ± 0.02 deduced in Ref. 2 using wedged samples. The discrepancy may have resulted from the use of wedged samples in Ref. 2.
[12]C. Kittel, *Quantum Theory of Solids* (Wiley, New York, 1963), Chap. 9; Eq. (3) is cast into a form so that it can be compared with results from a two-band calculation. It must be noted, however, that for Ge a two-band model does *not* correctly predict the magnitude and the anisotropy of the nonparabolicity, and that the numerical factors 1.4 and 0.8 in Eq. (3) actually result from the use of energy parameters for the eight bands at the L point.
[13]G. Dresselhaus and M. S. Dresselhaus, Phys. Rev. 160, 649 (1967); M. Cardona and F. H. Pollack, *ibid.* 142, 530 (1966), and references therein.
[14]H. Ehrenreich, J. Appl. Phys. 32, 2155 (1961).

PHYSICAL REVIEW B VOLUME 2, NUMBER 6 15 SEPTEMBER 1970

Luminescent Properties of Energy-Band-Tail States in GaAs:Si

D. Redfield, J. P. Wittke, and J. I. Pankove
RCA Laboratories, Princeton, New Jersey 08540
(Received 16 April 1970)

Several new properties which are characteristic of energy-band-tail states have been measured by transient photoluminescence in samples of GaAs heavily doped with silicon and partially compensated. Their dependence on temperature, doping and excitation intensity, and geometry has been determined. The primary results are the wide range (~ 100:1) of luminescent rise and decay times within the single emission band found at low temperatures, these times increasing monotonically with decreasing energy. These results are ascribed to the localized nature of band-tail states and to the necessary spatial separation of states in the tails of the valence and conduction bands. These observations also lead to the conclusion that thermalization times of the deeper band tails are very long – exceeding the carrier lifetimes, which reach several microseconds in some cases. Therefore, quasiequilibrium conditions do not develop in any of these experiments.

I. INTRODUCTION

Optical measurements have become very powerful aids to our understanding of both the intrinsic character of solids and the properties of defects within them. The present work is concerned with the nature of the luminescence associated with the presence of high concentrations of charged impurities in semiconductors. For this purpose, it has been found that GaAs: Si provides an interesting system. We regard it, however, as a convenient prototype; most of the conclusions reached here should apply to other cases of heavily doped semiconductors and certain disordered materials.

It is generally accepted that high concentrations of impurities in semiconductors create "tails" in the distribution of allowed states as a function of energy, these band tails extending into the normally forbidden gap.[1-6] The conditions which must be met for this description to be appropriate are (i) low binding energy of the impurities and (ii) impurity concentration high enough so that the spatially